RSC Advances

ROYAL SOCIETY OF CHEMISTRY

www.rsc.org/advances

Synthesis of Polyaniline/TiO_2 Composite with Excellent Adsorption Performance on Acid Red G

Ning Wang[a,b], Jingjing Li[b], Wei Lv[a,b], Jiangtao Feng[b]*, Wei Yan[a,b]*

[a]State Key Laboratory of Multiphase Flow in Power Engineering, Xi'an Jiaotong University, Xi'an 710049, PR China

[b]Department of Environmental Science and Engineering, Xi'an Jiaotong University, Xi'an 710049, PR China

*Corresponding authors: Wei Yan, State Key Laboratory of Multiphase Flow in Power Engineering, Xi'an Jiaotong University, Xi'an 710049, China, E-mail: yanwei@mail.xjtu.edu.cn; Jiangtao Feng, Department of Environmental Science and Engineering, Xi'an Jiaotong University, Xi'an 710049, China, E-mail: fjtes@mail.xjtu.edu.cn.

ABSTRACT

Polyaniline-modified TiO_2 (PANI/TiO_2) composite was designed and synthesized via the *in-situ* chemical polymerization of aniline monomer in the as-prepared TiO_2 sol solution. The composite was employed as a novel reusable adsorbent based on the unique doping/dedoping properties of polyaniline. Fourier transform infrared (FT-IR) spectra, scanning electron microscopy (SEM) and X-ray diffraction (XRD) were combined to characterize the chemical structure and morphology of PANI/TiO_2. The adsorption-desorption characteristics of polyaniline/TiO_2 (PANI/TiO_2) on Acid Red G (ARG) were further investigated. The prepared adsorbent possessed excellent adsorption and regeneration performances with the adsorption equilibrium time in about 5 min and the maximum adsorption capacity at 454.55 mg g^{-1}. The possible adsorption mechanism was proposed to be associated with the doping/dedoping behaviors of the PANI chain.

***Keywords*:** PANI/TiO_2 composite, adsorption, regeneration, Acid Red G

Introduction

In recent years, the composites of conductive polymers and inorganic particles have been the focus of a great deal of research[1-5] due to their potential applications in chemical sensing, catalysis, energy storage, solar cells, and medical diagnosis.[6-8] However, the application of this new type of materials as adsorbent in wastewater treatment, especially in the removal of dyes from printing and dyeing wastewater, is seldom reported.

Among conductive polymers (polyaniline, polypyrrole, polythiophene, etc.), polyaniline (PANI) has attracted

considerable attention for its low cost, simple synthesis, excellent electrical conductivity, thermal stability, antioxidant properties, and so on.[9-11] The unique reversible electrochemical activity, large specific surface area, good stability and doping-dedoping reversibility, etc.,[12, 13] make the adsorption and desorption of ions on PANI possible by simple acid and alkali treatment. The use of polyaniline as adsorbent for dye removal has been reported recently.[14, 15] However, PANI, as a significant conductive polymer material with low mass density, is hard to be settled, which restricts the application as the adsorbent for the difficulty of recovery.

Titanium dioxide is one of the most widely studied metal oxide semiconductor in the research of inorganic materials because of its comparatively low cost, simple preparation, good stability, nontoxic nature, and photodegradation ability.[16] Notably, the properties of insolubility and neutral pH_{pzc} value make TiO_2 an ideal adsorbent, and the adsorption capacity can be developed over a broad range of pH.[17] In addition, TiO_2 with large surface area[18, 19] carries a great deal of hydroxyl and carboxyl groups, which can interact with some pollutant molecules.[20-22] Recently, the adsorption of TiO_2 on various dyes, such as Acid Orange 7,[23] Porphyrin Dyes,[24] Esin Y Dye,[25] Blue 21 dye[26] and so on[27, 28] was reported. However, pure TiO_2 has high selectivity on the adsorbates and poor regeneration capability.[29] Therefore, the improvement in the adsorption and regeneration capability of TiO_2 through modification with other substances has been one of the focuses. And the modified substances would not decrease its adsorption capacity,[30] for the incompleted-OH groups on TiO_2 do not fully contribute to the ion exchange process.

Thus, the composites of PANI and TiO_2 were proposed in this study to develop the merits of both organic and inorganic materials and to avoid the shortcomings of both. We synthesized PANI-modified TiO_2 (PANI/TiO_2) composite through the chemical oxidation of aniline in the as-prepared TiO_2 sol solution, and investigated its adsorption and regeneration properties for Acid Red G (ARG). It was found that PANI/TiO_2 composite exhibited excellent adsorption and regeneration properties even after several adsorption-desorption cycles. Furthermore, compared with some other adsorbents reported before, the PANI/TiO_2 composite adsorbent exhibited excellent adsorption performance for ARG and could reach the adsorption equilibrium in a very short time. Finally, a possible adsorption mechanism was proposed according to the doping/dedoping behaviors of the PANI.

Experimental

Materials

Aniline (99.5%, Sinopharm Chemical Reagent Co., Ltd, Shanghai, China) was distilled twice under reduced pressure, and then stored in the dark at 0 ^{o}C protected by N_2. Acid Red G (ARG) was commercial grade and recrystallized twice before used. The structure of ARG is shown in Fig. 1. Other reagents were of analytical grades and used as received. The real effluent used in our study was derived from the printing and dyeing factory in Xi'an, China. The deionized water used for all the experiments was prepared by an EPED-40TF Superpure Water System (EPED, China).

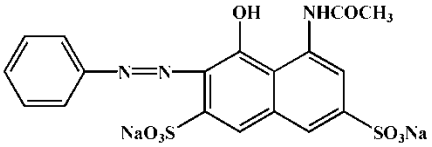

ARG

Fig.1. Molecular structure of ARG

Synthesis of the PANI/TiO_2 composite

The TiO_2 sol solution was prepared by the sol-gel hydrolysis[15] in the mixture solution of HNO_3 (0.064 mol L^{-1}) and citric acid (0.1 mol L^{-1}), in which PANI/TiO_2 was formed by the chemical oxidative polymerization of aniline monomer. The typical process is as follows: the dispersed TiO_2(2.35 g) in 100 mL mixture solution of HNO_3 (0.064 mol L^{-1}) and citric acid (0.1 mol L^{-1}) was magnetically stirred for 1.0 h. Afterwards, aniline (1.8 mL) monomer was added and stirred for 1 h. Then, ammonium persulphate (APS) solution (0.1 mol L^{-1}) was added and reacted for 8 h at ambient temperature. Finally, the composite was filtrated and washed with a large amount of deionized water and dried at 50 ^oC for 48 h. For comparison, the pure TiO_2 and PANI were prepared as above.

Characterization

XRD patterns of the samples were obtained by an X'Pert PRO MRD Diffractometer using Cu-Kα radiation (λ=1.5418 Å). FT-IR spectra of samples were measured using the KBr pellet method on a BRUKER TENSOR 37 FT-IR spectrophotometer in the range of 4000-400 cm^{-1}. The Brunauer-Emmett-Teller surface area (S_{BET}), total pore volume (V), and average pore radius (R) were determined by the ASAP2020 instrument using the Barrett-Joy-ner-Halenda (BJH) method. The thermogravimetric analysis (TGA) was performed on a Perkin Elemer TGA-7 in N_2 flow at heating rate of 10 ^oC min^{-1}. The morphology was characterized by scanning electron microscopy (SEM, JSM-6700F, Japan; JJSM-6390A, JEOL instrument). The zeta potentials of adsorbents were measured with Malvern Zetasizer Nano ZS90, through adding 5 mg sample in 10 mL NaCl solution (10^{-3} mol L^{-1}) at different pH values (adjusted with diluted HNO_3 or NaOH solution).

Adsorption Experiments

All adsorption experiments were carried out in the dark at ambient temperature. The suspension containing 500 mg L^{-1} ARG and PANI/TiO_2 adsorbent was magnetically stirred for a certain time and then centrifuged at 4000 rpm for 2 min. The supernatant was analyzed by the UV-Vis spectrophotometer (Agilent 8453) and the adsorption intensity peak at 503 nm corresponding to the azo group in Acid Red G was recorded, with which the concentration of ARG in solution can be calculated.

The influence of the pH on the adsorption capacities was investigated by adjusting the pH of ARG solution with NaOH or HNO_3 solution (pH=1.0-13.0). Then the adsorbents were employed to treat ARG solutions with different pH. Due to the complexity of real effluent, the effect of ionic concentration on the adsorption was also conducted by adding NaCl (0-0.3 mol L^{-1}) into the 500 mg L^{-1} ARG solution before the adsorption process. The optimal dosage of PANI/TiO_2 in the adsorption was determined by varying the adsorbent concentration from 0.5 to

3.0 g L^{-1}. The thermodynamics of the prepared adsorbent was examined by changing the adsorption temperature from 10 to 35 ^{o}C.

The adsorption equilibrium of different concentrations of ARG (300, 500, and 700 mg L^{-1}) on PANI/TiO_2 was evaluated at 20 ^{o}C, with the optimal dosage of PANI/TiO_2 in 1 h. 10 mL of the mixture was fetched in the same time interval (10 min) and filtered for the UV-Vis spectrophotometer analysis at λ_{max}=503 nm.

The adsorption rate R (%) and the amount of adsorbed dye on per gram of adsorbent (Q_t (mg g^{-1})) in time *t* were calculated by the following equations, respectively:

$$R(\%) = \frac{C_0 - C_t}{C_0} \times 100 \qquad (1)$$

$$Q_t(mg/g) = \frac{C_0 - C_t}{M} \times V \qquad (2)$$

where: C_0 is the initial dye concentration (mg L^{-1}), and C_t is the concentration of dye adsorbed in time t; V is the solution volume (L) and M is the mass of the used adsorbent (g).

To determine the maximum adsorption capacity and the suitable isotherm model of the adsorbents for ARG (500-950 mg L^{-1}), the Langmuir and Freundlich isotherm models were selected to fit with the experimental data at 20 ^{o}C. Langmuir and Freundlich isotherms are described in the following equations, respectively:

$$\frac{C_{eq}}{Q_{eq}}(g/L) = \frac{1}{Q_{max} K_L} + \frac{C_{eq}}{Q_{max}} \qquad (3)$$

$$\lg Q_{eq}(mg/g) = \lg K_F + n \lg C_{eq} \qquad (4)$$

where: Q_{eq} and Q_{max} (mg g^{-1}) are the equilibrium adsorption capacity and the maximum adsorption capacity, respectively; C_{eq} (mg L^{-1}) is the dye equilibrium concentration in the solution; K_L (L mg^{-1}) is a constant that relates to the heat of adsorption; K_F ((mg g^{-1}) (mg $L^{-1})^{-n}$) represents the adsorption capacity when C_{eq} equals 1; *n* represents the degree of dependence of adsorption on equilibrium concentration.

Regeneration Experiments

Due to the reversible doping/dedoping chemistry of PANI and the neutral pH_{pzc} value of TiO_2, the as-prepared composites can be regenerated by simple acid and alkali treatment theoretically. Therefore, 0.1 mol L^{-1} NaOH and 0.1 mol L^{-1} HCl solutions were used to treat the PANI、TiO_2 and PANI/TiO_2 for 10 min sequentially. Then the regenerated adsorbent was reused for the adsorption experiments. The adsorption rate and adsorption capacity of regenerated adsorbents were calculated by eq. (1) and (2).

The real ARG effluent was prepared by dissolving ARG (500 mg L^{-1}) into the real effluent instead of deionized water. The adsorption experiments of ARG effluent were the same as that of ARG solution.

Results and discussion

Characterization of the Samples

The chemical structure of PANI/TiO_2 was characterized by FT-IR spectroscopy in Fig. 2. The broadband centering at about 3300 cm^{-1} could be assigned to the stretch vibration of O-H and N-H groups on the surface of TiO_2 and in the chains of PANI. In the spectrum of TiO_2, the wide peak at 500-700 cm^{-1} corresponds to Ti-O-Ti bending mode of TiO_2.[31] The bands at 1631, 1560, and 1237 cm^{-1} are assigned to the O-H stretch vibration, the O-C=O asymmetric stretch vibration, and the C=O stretch vibration from the doped citric acid respectively. In addition, the peak at 1388 cm^{-1} is assigned to the N-O stretching vibration introduced by nitrate ion from synthesis. In the spectrum of PANI, the characteristic peaks at 1577, 1502, 1301, and 827cm^{-1} are ascribed to the C=C stretching vibration of quinoid and benzenoid rings, C-N stretching of -NH-(C_6H_4)-NH- and C-H vibration out of benzene plane ring respectively.[32, 33] A wide peak at 1141 cm^{-1} assigned to the Q=NH^+-B adsorption peaks (where Q and B denote quinoid ring and benzene ring, respectively) is also observed.[34] All the main characteristic bands of PANI and TiO_2 can be seen in the spectrum of PANI/TiO_2. The slight shift of characteristic peaks at 1577 and 1502 cm^{-1} might be caused by the chemical interaction between the amine groups or the imine groups of the PANI chains and the TiO_2. The reaction occurred on the basis that titanium as transition metal has intense tendency to form coordination compound with nitrogen atom in PANI macromolecule. This interaction as reported may weaken the bond strengths of C=N, C=C and C-N in PANI macromolecule,[35, 36] which can be confirmed by comparing the peak intensity of PANI and PANI/TiO_2.

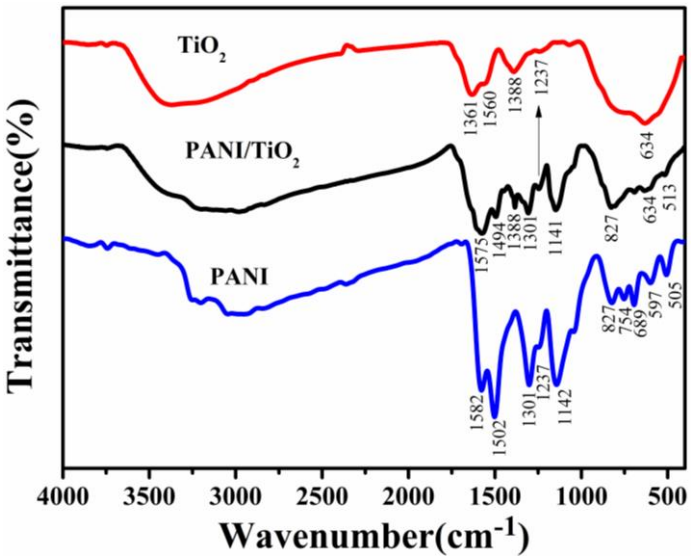

Fig. 2. FT-IR spectra of TiO_2, PANI/TiO_2, and PANI samples.

According to Geniès,[37] the peak intensity ratio of quinoid and benzenoid structure (I_Q/I_B) in PANI is related to the degree of oxidation in the molecular chain. In Fig. 2, the I_Q/I_B ratio in the spectrum of PANI/TiO_2 and PANI were calculated by integrating the corresponding peaks area. A big change occurred for the I_Q/I_B ratio, 0.96 for PANI and 9.31 for PANI/TiO_2, suggesting significant increase of the oxidation degree in PANI molecule chain after the composition with TiO_2. The relation between the I_Q/I_B ratio and the adsorption would be discussed later.

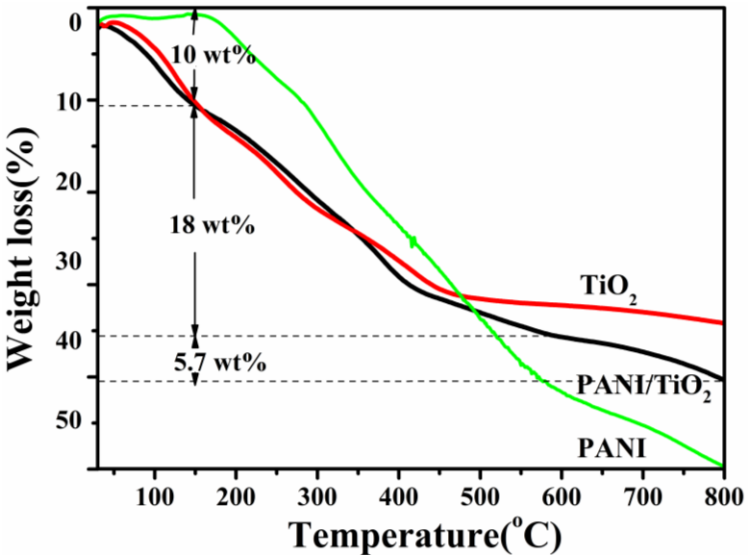

Fig. 3. TGA curves of TiO_2 and PANI/TiO_2.

Fig. 3 depicts the TGA curves of PANI/TiO_2, PANI and TiO_2. It can be seen that the weight loss of PANI occurred from 180 °C and lasted in the whole procedure with weight loss of 55 wt%. The weight loss of PANI/TiO_2 was similar to that of TiO_2 and showed a three-stage decomposition pattern. The first weight loss of PANI/TiO_2 and TiO_2 at temperature below 150 °C was attributed to desorption of water and anions inherited from the synthesis process.[38] The major thermal event between 150-580 °C with about 18 wt % of weight loss may be assigned to the hydroxyl condensation dehydration on TiO_2 and degradation of PANI. Above 300 °C, the weight of PANI/TiO_2 decreased faster than that of TiO_2, indicating the thermal degradation of PANI.[39] The last weight loss of 5.7 wt% above 580 °C in PANI/TiO_2 was attributed to further degradation of PANI. Comparing the TGA curve of PANI/TiO_2 and PANI, the as-prepared PANI/TiO_2 possessed higher thermal stability than PANI after the composition with TiO_2.

The morphologies of the prepared TiO_2, PANI and PANI/TiO_2 were investigated by SEM in Fig. 4. It can be seen that PANI showed peculiar flake aggregation in Fig. 4a. Pure TiO_2 was spherical with uniform diameter under 500 nm (Fig. 4b). It can be seen from Fig. 4c that the composite PANI/TiO_2 was spherical with 1 μm of average diameter, which is much different with the PANI flake. It is indicated that the composition with TiO_2 could significantly change the morphology of PANI. The increase of the average diameter of PANI/TiO_2 is possibly due to the aggregation of PANI on TiO_2 surface.

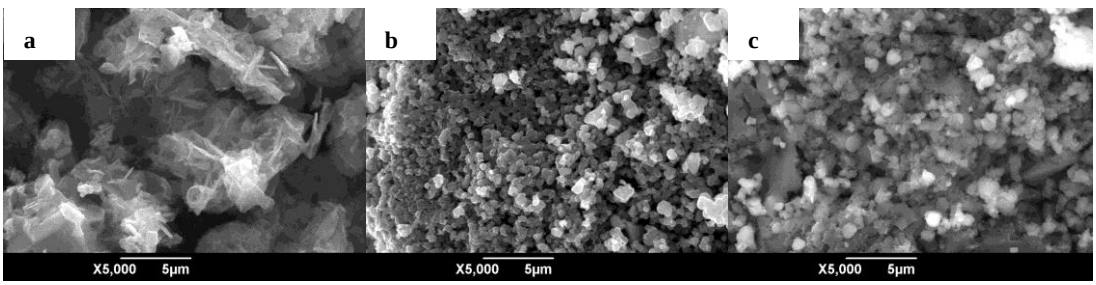

Fig. 4. SEM images of the prepared (a) PANI, (b)TiO_2 and (c) PANI/TiO_2.

Fig. 5 shows the XRD patterns of the prepared TiO_2, PANI and PANI/TiO_2. For TiO_2, only a weak diffraction peak located at about 25.4° corresponding to the anatase TiO_2 (101) plane[40] was observed, indicating the amorphous state of TiO_2 prepared by the sol-gel method. The characteristic peaks of the doped PANI at around 20.0° and 25.7° attributed to the periodicity parallel and perpendicular to the polymeric chain[41, 42] were observed, suggesting obvious crystallinity in the prepared PANI. While in the pattern of PANI/TiO_2, the diffraction peak of the PANI at about 25.3° decreased significantly, suggesting the prepared adsorbent was amorphous. It was reported that when the polyaniline deposits on the surface of TiO_2 particle, the molecular chain of absorbed polyaniline is tethered and the degree of crystallinity decreases,[43] which is consistent with this study, and corresponds to the result of SEM.

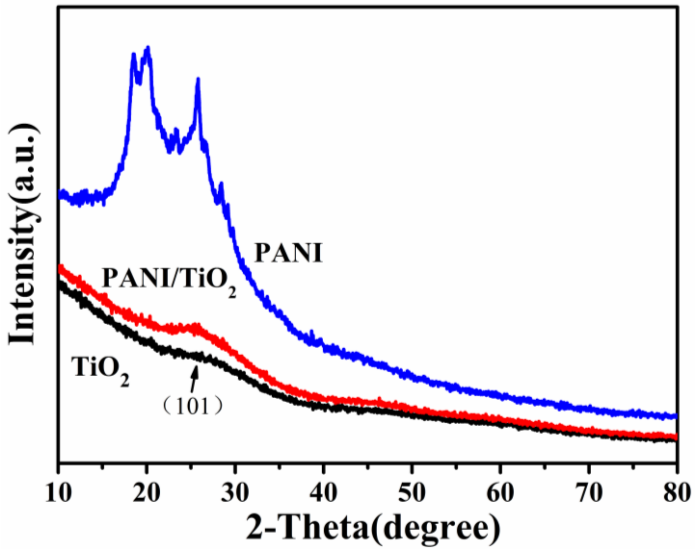

Fig. 5. XRD patterns of the prepared TiO_2, PANI and PANI/TiO_2.

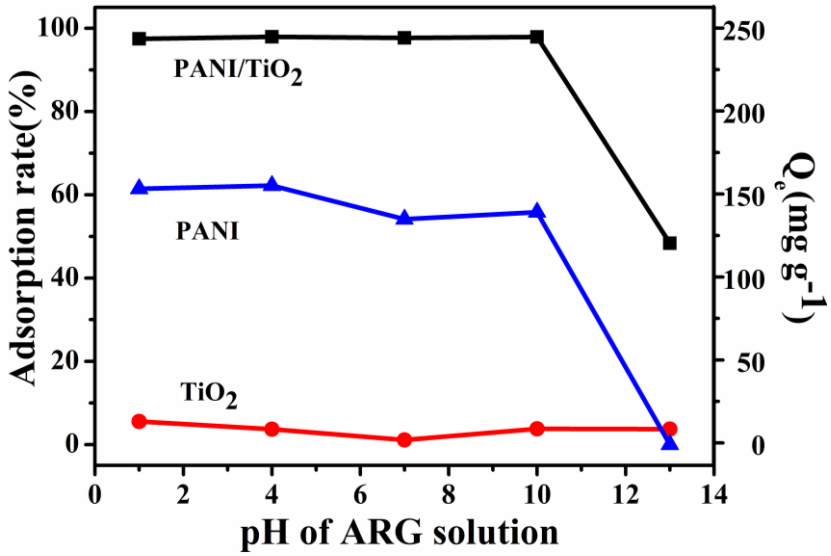

Fig. 6. Effect of pH on adsorption capacities of the prepared samples.

Effects of pH and Ionic Concentration on Adsorption

The effect of pH on adsorption capacities of the prepared PANI, TiO_2 and PANI/TiO_2 is shown in Fig. 6. It can be observed that TiO_2 exhibited extremely low capacity for dye removal in studied pH range. The adsorption rate of the PANI/TiO_2 was maintained more than 95% below pH 10, and was reduced to 55% at pH 13, indicating the adsorption of ARG occurred mainly on the PANI. In contrast, the plot of the PANI is similar to that of PANI/TiO_2 with lower adsorption rate (about 57% at pH lower than 10, and 0% at pH 13), suggesting that the composition of TiO_2 significantly increased the dye removal efficiency of PANI in the whole employed pH range. Actually, the performance difference of PANI and PANI/TiO_2 was mainly caused by the loss of PANI with low mass density which is hard to be settled, in the pre-treatment of the adsorbents. TiO_2 in the composition increased the settleability of the adsorbent thus increasing the adsorption and regeneration efficiency.

In order to analyze this phenomenon, zeta potentials of PANI, TiO_2, and PANI/TiO_2 at different pH values were measured and the results are shown in Fig. 7. At the zero zeta potential, the pH (labeled as pI) of PANI, TiO_2, and PANI/TiO_2 was 10.29, 2.13, and 3.37 respectively, suggesting that the composition of TiO_2 changed the zeta potentials of PANI. The change may be caused by two aspects: 1) the more negative surface potential of TiO_2 compared with the positive surface potential of the PANI, 2) the different dosages of TiO_2 (2.35 g) and PANI (1.83 g) in the composite. Due to these two aspects, the zeta potential of PANI/TiO_2 was changed and different with that of PANI. As for PANI, at pH below pI, nitrogen atoms, mainly on the imine groups, which are easier to be protonated than the amine groups,[44, 45] are protonated, making the PANI carry positive charges. When the pH is above pI, PANI/TiO_2 is negatively charged due to competitive adsorption of OH^- anions on both imine and amine functional groups.[46, 47] When the adsorbents are positively charged, the anionic dye can be easily adsorbed through the electrostatic attraction. If the adsorbents are negatively charged, the electrostatic repulsion inhibits the adsorption of ARG molecules. The results of PANI and TiO_2 were consistent with the change of adsorption capacities at different pH. However, although the pI was 3.37, the prepared PANI/TiO_2 showed excellent adsorption efficiency in the pH range of 1-10, which indicated that the adsorption of PANI after composed with TiO_2 was not just dominated by electrostatic attraction.

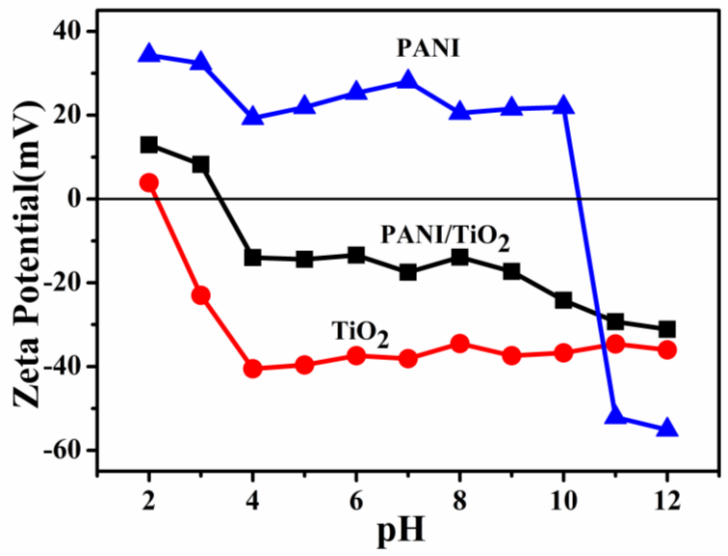

Fig. 7. Zeta potentials of samples.

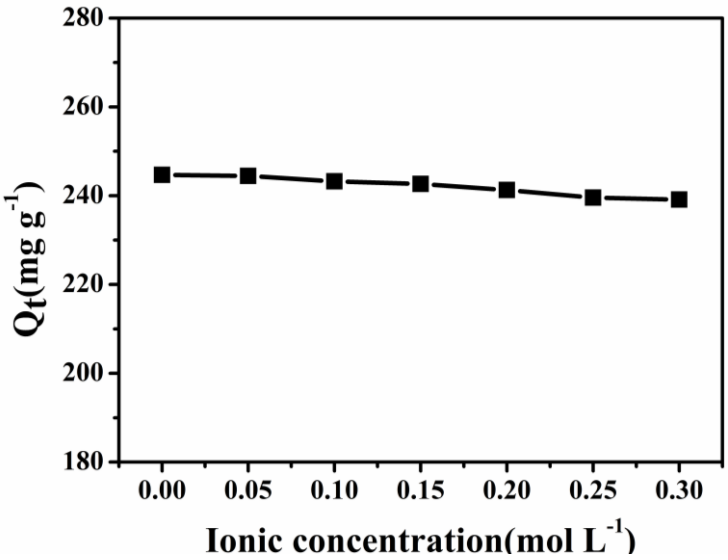

Fig. 8. Effect of ionic concentration on the adsorption capacity of PANI/TiO_2.

(NaCl (0-0.3 mol L^{-1}) was added into the 500 mg L^{-1} ARG solution before the adsorption process)

Generally speaking, the real effluent from printing and dyeing factories is quite complex.[48] Therefore, the study on the effect of ionic concentration on the adsorption capacity was necessary and the result is shown in Fig. 8. It was found that the inhibition of ionic concentration on adsorption capacity was tiny. According to Zhang *et al.*,[49] on the one hand the ions can reduce the electrostatic attraction between the adsorbates and adsorbents, but on the other hand they can inhibit the electrostatic repulsion between the adsorbates. With these two aspects, the adsorption capacity of PANI/TiO_2 remained invariable with the change of ionic concentration.

Effects of Adsorbent Dosage and Temperature on Adsorption

In order to determine the optimal dosage of PANI/TiO_2 in application, the effect of PANI/TiO_2 dosage on the adsorption for ARG was studied and the result is shown in Fig. 9a. According to Fig. 9a, the adsorption efficiency increased consequently with the increase of dosage. The adsorption efficiency showed no obvious change when the

dosage exceeded 2.0 g L^{-1}. As a result, the dosage of 2.0 g L^{-1} was chosen in the subsequent experiments.

Fig. 9b shows the influence of temperature on adsorption at 10 ^{o}C, 20 ^{o}C and 35 ^{o}C. It can be seen that there is no significant fluctuation on the adsorption behaviors when the temperature was changed, which indicated that the adsorption of ARG on PANI/TiO_2 was temperature independent in the range of 10-35 ^{o}C.

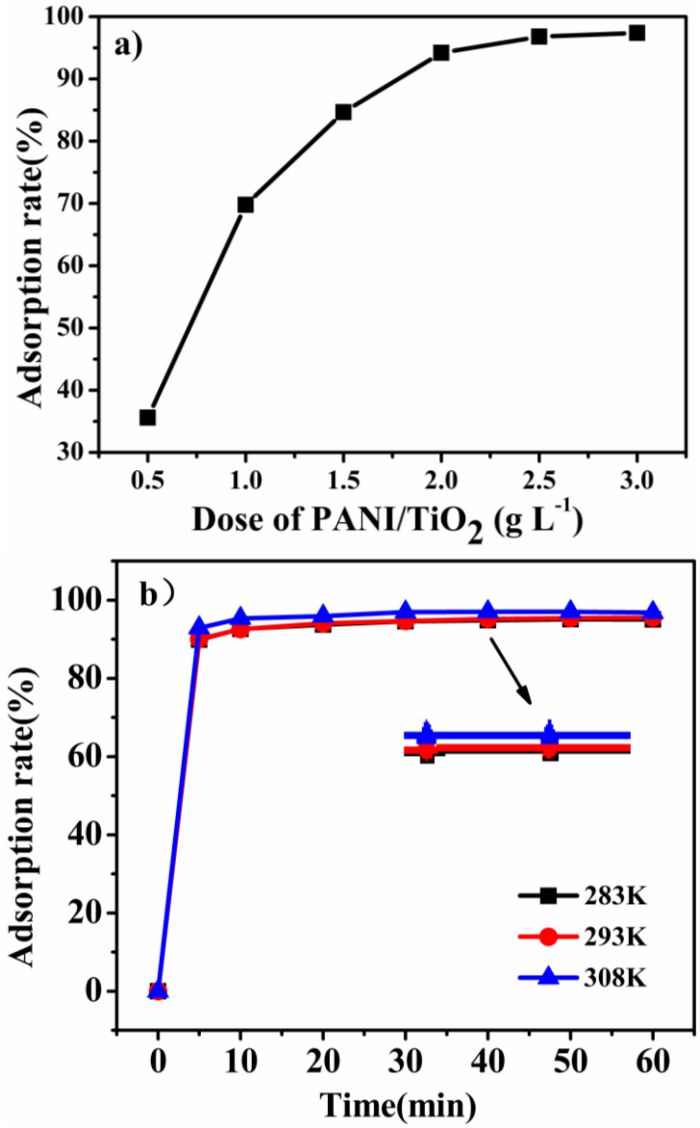

Fig. 9. Effects of PANI/TiO_2 dosage(a) and temperature (b, insertion is a partial enlargred drawing) on the adsorption of ARG.

Adsorption Kinetics

Fig. 10 shows the adsorption kinetics of ARG on PANI/TiO_2. Fig. 10a depicts the influence of contact time on the adsorption of ARG on PANI/TiO_2 with different initial concentrations (300, 500, 700 mg L^{-1}). Evidently, the adsorption equilibrium of ARG on PANI/TiO_2 could be achieved in 5 min, which was much shorter than that of other adsorbents reported in literatures (listed in Table 3), indicating the as-prepared PANI/TiO_2 was a promising excellent adsorbent.

The adsorption kinetics of ARG onto PANI/TiO_2 was analyzed by the Pseudo-First-Order and

Pseudo-Second-Order Models which are described in eqs. (5) and (6), respectively. The results are illustrated in Fig. 10b, c.

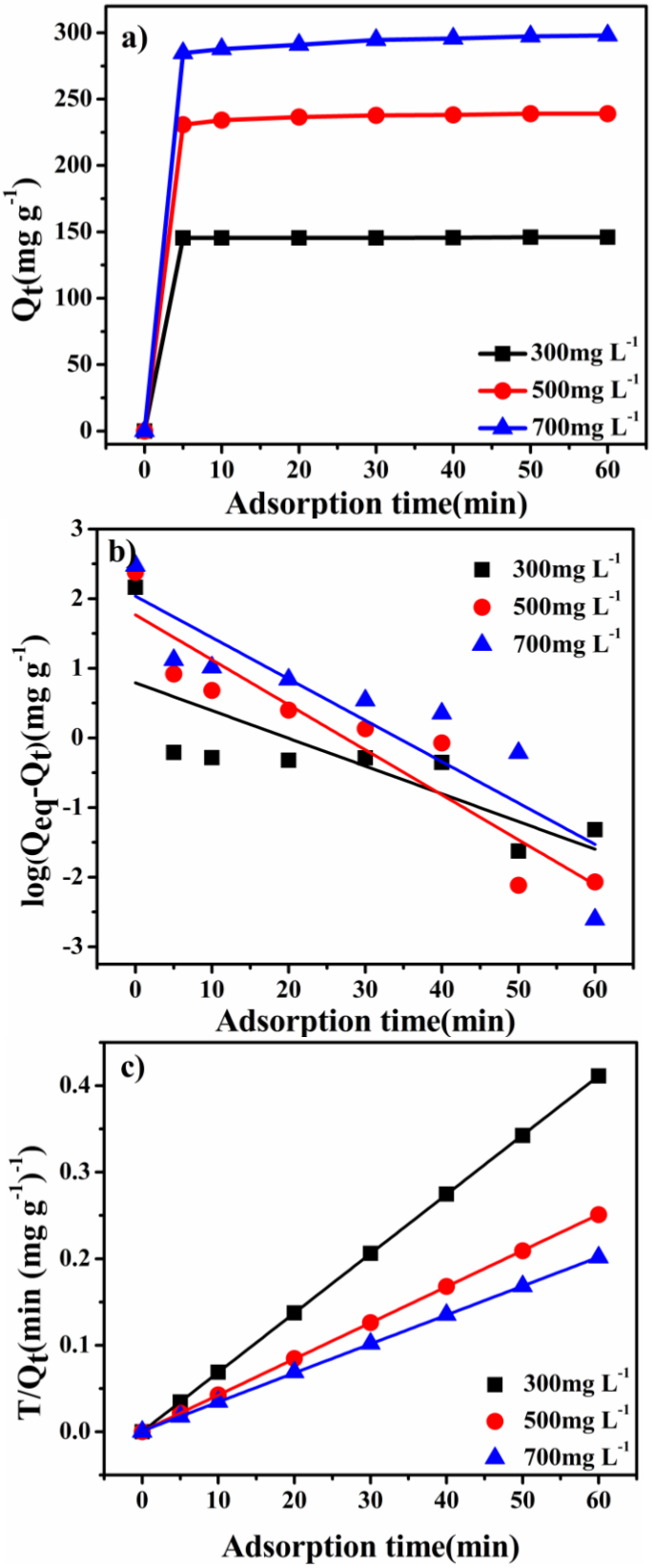

Fig. 10. Adsorption equilibrium curves of ARG onto PANI/TiO_2 (a); Pseudo-first-order kinetic plot for the adsorption of ARG(b); and Pseudo-second-order kinetic plot for the adsorption of ARG(c).

$$\lg\left(Q_{eq}-Q_t\right)=\lg Q_{eq}-\frac{K_1}{2.303}t \qquad (5)$$

$$\frac{t}{Q_t}=\frac{1}{K_2Q_{eq}^2}+\frac{t}{Q_{eq}} \qquad (6)$$

where t is the adsorption time (min), K_1 (min^{-1}), and K_2 (g mg^{-1} min^{-1}) are the rate constants for the pseudo-first-order and pseudo-second-order models, respectively. Q_{eq}(mg g^{-1}) is the equilibrium adsorption capacity. Q_t (mg g^{-1}) is the adsorption capacity at t min.

The relevant parameters of the pseudo-first-order and pseudo-second-order models were calculated and are listed in Table 1. The validity of kinetic model can be evaluated by two factors: the correlation coefficients (R^2) and the agreement of experimental data and calculated data.[50] It can be observed that the correlation coefficients of the pseudo-second-order model (R^2=0.9999-1) was more appropriate to describe the adsorption kinetics of PANI/TiO_2 for ARG than the pseudo-first-order model (R^2=0.6342-0.7119), which was consistent with most adsorbents reported.[51, 52] Moreover, the calculated values of Q_{eq} from the pseudo-second-order model agreed well with the experimental data. Therefore, the adsorption kinetics of ARG on PANI/TiO_2 followed the pseudo-second-order model, indicating the multiple adsorption mechanism of the PANI/TiO_2 adsorbent with saturated sites.[53]

Table 1

Parameters of the Pseudo-First-Order and Pseudo-Second-Order Models.

C_0 (mg L^{-1})	Pseudo first order model			Pseudo second order model		
	K_1(min^{-1})	Q_{eq} (mg g^{-1})	R^2	K_2(g mg^{-1} min^{-1})	Q_{eq} (mg g^{-1})	R^2
300	0.0532	1.208	0.5318	0.1156	144.93	0.9999
500	0.1985	74.456	0.8589	0.0176	238.10	0.9999
700	0.1658	137.911	0.7638	0.0078	303.03	1

Adsorption Isotherms

Adsorption isotherms, as empirical models, are obtained from the experimental data by means of regression analysis and are often used to describe the equilibrium of the sorption at constant temperature. The most common isotherms are the Freundlich isotherm and the Langmuir isotherm. Fig. 11 depicts the linear forms of Langmuir and Freundlich adsorption isotherm models of PANI/TiO_2. Evidently, the degree of linearity of Langmuir adsorption isotherm model was better than that of Freundlich adsorption isotherm model. The parameters of Freundlich and Langmuir isotherm models are listed in Table 2. It was found that the adsorption behaviors of ARG on the PANI/TiO_2 sample followed the Langmuir adsorption isotherm, suggesting the adsorption process was a monolayer adsorption.

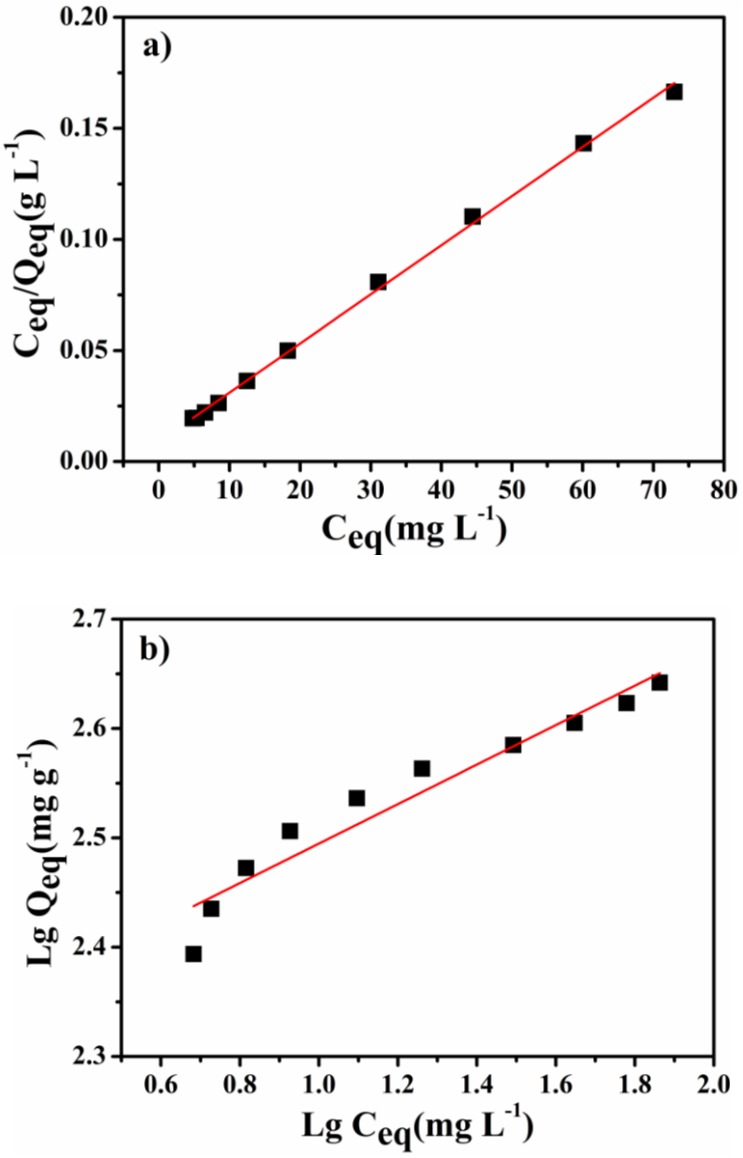

Fig. 11. Liner forms for (a) Langmuir and (b) Freundlich isotherm model of ARG onto PANI/TiO_2.

Table 2

Parameters of Langmuir and Freundlich Adsorption Isotherm Models.

Langmuir model				Freundlich model		
Q_{max} (mg g^{-1})	K_L(L mg^{-1})	R_L	R^2	K_F((mg g^{-1})(L mg^{-1})$^{-n}$)	*n*	R^2
454.55	0.25	0.0042	0.9985	206.2	0.18	0.9346

The dimensionless separation factor, R_L, which is used to study the applicability of Langmuir adsorption isotherm, is expressed in the following equations:

$$R_L = \frac{1}{1+bC_0} \quad (7)$$

where, C_0 is the initial concentration of ARG solution; b is Langmuir constant.

The adsorption process is irreversible when R_L=0, favorable when 0<R_L<1, linear when R_L=1, and unfavorable when R_L > 1.[54, 55] The R_L value here was calculated as 0.0041 for the adsorption of ARG, in the range of 0-1, indicating the process of ARG adsorbed on PANI/TiO_2 is favorable.

The largest adsorption amount of ARG onto PANI/TiO_2 composite derived from the Langmuir model was 454.55 mg g^{-1}, which was much higher than that of several other adsorbents reported in literatures (listed in Table 3). In addition, PANI/TiO_2 composites were also highlighted with the shorter equilibrium adsorption time than that of other adsorbents, suggesting that the PANI/TiO_2, a composite of conductive polymers and inorganic particles, possessed higher adsorption capacity for ARG dye, and was a promising adsorbent for the removal of anion dyes from wastewater.

Table 3

Adsorption capacity of PANI/TiO_2 and other adsorbents for Azo Dyes.

Adsorbents	Acid Red dyes	Q_{max} (mg g^{-1})	C_0 (mg L^{-1})	Equilibrium time (min)
PANI/TiO_2	Acid Red G	454.55	500	5
PPy/TiO_2[2]	Acid Red G	179.21	500	20
Activated carbon[56]	Acid Red 97	52.08	30	30
$CuFe_2O_4$ powder[57]	Acid Red B	86.8	100	30
Montmori llonite[58]	Acid Red G	171.53	300	60
Calcined-Alunite[59]	Acid Red 57	80.02	250	120
PANI-ES[60]	Alizarine Cyanine Green	56.00	175	60
PANI/Iron Oxide[61]	Amido Black 10B	61.72	80	150

Regeneration

Given the effect of pH and surface potential on the adsorption, the regeneration of PANI/TiO_2 was achieved by using NaOH solution (0.1 mol L^{-1}) as desorption agent and HCl solution (0.1 mol L^{-1}) as the activation agent. Repeatedly, the regenerated adsorbents were utilized to treat the same concentration of ARG solution, and the adsorption/regeneration stability was studied. Fig. 12 shows the adsorption/regeneration efficiency of PANI/TiO_2 for ARG solution (500 mg L^{-1}) and real ARG effluent (actual printing and dyeing wastewater containing 500 mg L^{-1} ARG).

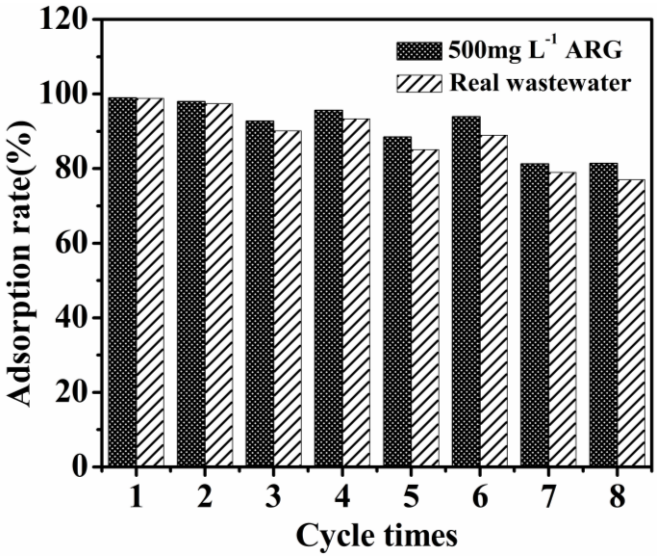

Fig. 12. The adsorption/regeneration efficiency of PANI/TiO_2 for ARG solution and real ARG effluent.

As for the ARG solution, it can be observed that the adsorption rate slightly decreased, resulting from the incomplete stripping of ARG on PANI/TiO_2 and also the inevitable loss of adsorbents. In contrast, the adsorption efficiency for actual printing and dyeing wastewater containing 500 mg L^{-1} ARG is less than that for pure ARG solution and showed a continuously decrease trend, which may be due to the complexity of actual dyeing wastewater. In spite of 8 cycles of adsorption/regeneration, the adsorption efficiency for ARG solution was still more than 80%. Additionally, for the real ARG effluent, the adsorption efficiency of PANI/TiO_2 was more than 77% after 8 times of regeneration. These results suggested that the PANI/TiO_2 composite can be regenerated by acid and alkali treatment and the adsorption stability were hardly affected.

For comparison, the regeneration of PANI and TiO_2 was also studied. According to the experimental result, the regeneration efficiency of PANI and TiO_2 were both much lower than that of PANI/TiO_2, almost negligible. For PANI, it resulted from the inevitable loss of the suspended PANI during desorption and activation process. And for TiO_2, titanium hydrates as the main constituents of TiO_2 were very unstable to acid and would dissolve in 0.1 M HCl during the acid activation process, seriously restricting the regeneration of TiO_2. The results indicated that the composition of PANI and TiO_2 could significantly increase the regeneration capacity of the adsorbent.

A Proposed Adsorption Mechanism

The possible adsorption mechanism may be related to the unique doping-dedoping behaviors of PANI in the PANI/TiO_2, where the ARG ions can be served as the dopants ions. In order to study the proposed mechanism of adsorption and subsequent removal of the dye ARG, the FTIR of the samples treated by different conditions were measured(Fig. 13). In Fig. 13, the PANI/TiO_2 is the prepared adsorbents without any treatment; Alkali-PANI/TiO_2 is the prepared adsorbent treated by alkali(0.1 M NaOH); Acid-PANI/TiO_2 is the Alkali-PANI/TiO_2 treated by acid(0.1M HCl); and the Ad-PANI/TiO_2 is the Acid-PANI/TiO_2 after the adsorption for ARG.

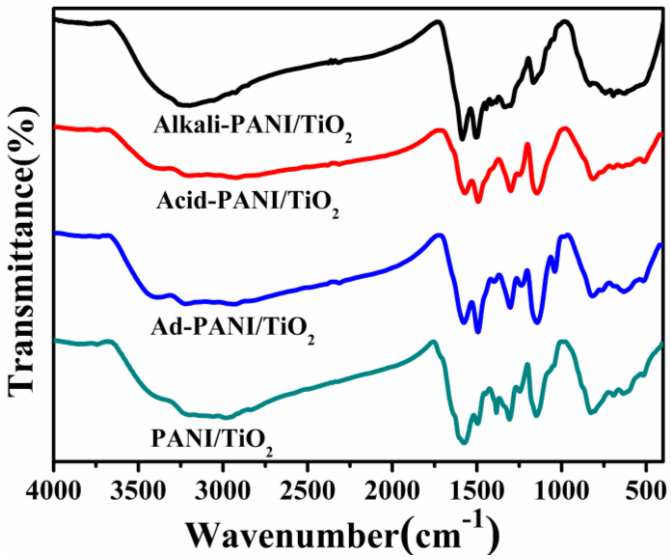

Fig. 13. FT-IR of Alkali-PANI/TiO_2, Acid-PANI/TiO_2, Ad-PANI/TiO_2, and PANI/TiO_2.

From the Fig.13, it can be found that there appeared a new peak at about 1047 cm^{-1} in the FT-IR spectra of Ad-PANI/TiO_2 sample, which is attrbuted to S=O stretching vibration in ARG dye.[62] We deduced that ARG dye may served as the dopant ions in the PANI chain during the adsorption, i.e. pronotation, process. Here, the change of I_Q/I_B in different samples was studied because the doping degree of the PANI chain was reported to be associated with the I_Q/I_B ratio.[63, 64] The I_Q/I_B ratio in the spectrum of the four samples were calculated, and the results are listed in Table 4.

Table 4

The I_Q/I_B ratio in the spectrum of the four samples.

Samples	I_Q/I_B	Adsorption rate(%)
PANI/TiO_2	9.31	44
Alkali-PANI/TiO_2	2.94	13
Acid-PANI/TiO_2	1.52	98
Ad-PANI/TiO_2	1.75	--

It can be seen from Table 4 that the I_Q/I_B ratio in prepared PANI/TiO_2 was the highest, indicating the largest content of quinoid units, which maybe result from the oxidation of APS whose hydrolysis products include H_2O_2. After the alkali treatment, the I_Q/I_B ratio decreased dramatically; the alkali treatment was considered as dedoping process. However, the value of the I_Q/I_B ratio (2.94) indicated the incomplete dedoping in the PANI chain. And then the I_Q/I_B ratio fell to 1.52 after the acid treatment, indicating the acid dual-doping resulted in the transfer of electron and the change of electron cloud.[65] No big change happened on the ratio after the adsorption. According to the doping behaviors of the PANI reported[65] and the results in Table 4, the possible adsorption process can be

deduced as follows in Fig. 14:

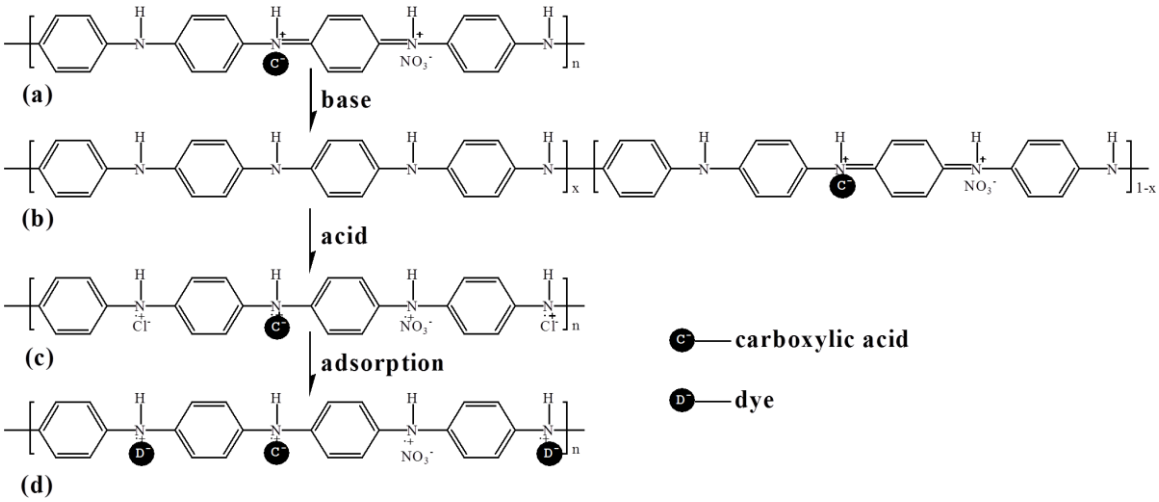

Fig. 14. the proposed doping process and adsorption procedure

As shown in the Fig. 14, the prepared PANI in the composites was mainly in the emeraldine oxidation state (PANI-ES) with dopant of nitrate and citrate ions on the imine nitrogen atoms in the preparation process (Fig. 14a). In this state, the adsorption rate (in Table 4) was only 44%, which happenned mainly on the protonated imine N atoms with the replacement of nitrate and citrate ions by dye ions. When the composites was treated with NaOH, parts of nitrate and citrate ions were released by charge neutralization and the corresponding PANI chain backbone transformed from quinoid into benzenoid units[47] with the decrease in the I_Q/I_B ratio; this process can also be considered as dedoping with NaOH. However, according to the Fig. 13 and Table 4, there still existed nitrate and citrate ions characteristic peaks (at 1388 and 1237 cm^{-1}) and the I_Q/I_B ratio was 2.94 for Alkali-PANI/TiO_2. Therefore, it can be indicated that parts of quinoid units with dopant existed in the chain, and the structure of the PANI chain may be like Fig. 14b. The lowest adsorption rate at this state resulted from the small amount of protonated N atoms in this state, decreasing the substitution reaction of the counter ions on it. Then the chain of PANI was re-protonated with the excess HCl acid,[66, 67] resulting more protonated nitrogen atoms in the PANI chain and less quinoid units because of the electron transfer and the change of electron cloud. In the adsorption process, the re-protonated PANI chain attracted the anion dye through electrostatic adsorption, and the replacement of Cl^- ions with dye anions occurred because of the stronger electrostatic adsorption force and the concentration grads (see Fig. 14d and the FT-IR spectra of Ad-PANI/TiO_2 in Fig. 13).

Table 5

Surface property of Different Samples.

Samples	$S_{BET}(m^2\ g^{-1})$	$V(cm^3\ g^{-1})$	R(nm)
TiO_2	4.12	0.027	13.20

PANI	21.28	0.171	16.11
PANI/TiO_2	4.69	0.043	18.50
Alkali-PANI/TiO_2	3.055	0.018	11.91
Acid-PANI/TiO_2	2.052	0.020	19.90
Ad-PANI/TiO_2	30.61	0.067	4.39

The surface properties of samples treated by different reagents were measured and the results are listed in Table 5. From Table 5, the prepared PANI/TiO_2 showed small S_{BET}, and the alkali and acid treatment decreased the S_{BET}, which may be the result of the chemical corrosion by alkali and acid. After the adsorption, the S_{BET} increased and the R decreased significantly, suggesting the aggregation of ARG on the adsorbents surface and into the pore. Interestingly, it can be indicated from Fig. 6, Table 4 and Table 5 that the adsorption efficiency had nothing to do with the specific surface area, but showed a positive correlation with the pore radius, which was inconsistent with the traditional concept that adsorbent with larger surface area show high dye removal rate.

Conclusions

In this study, a novel composite adsorbent, PANI/TiO_2, was successfully synthetized. The formation of the PANI/TiO_2 composite was confirmed by XRD, FT-IR and SEM analysis. It was found that the PANI/TiO_2 was spherical structure with weak crystallinity. There existed certain interaction between PANI and TiO_2 according to the FT-IR. The TGA analysis showed that the amount of PANI composited in PANI/TiO_2 was close to 18 wt% and the PANI/TiO_2 possessed high thermal stability. According to the adsorption characteristics of ARG on PANI/TiO_2, it was found that PANI/TiO_2 composite performed excellent adsorption capability after acid treatment, with adsorption efficiency of more than 90% for 500 mg L^{-1} ARG solution. Although the effect of ion concentration on adsorption was negligible, the influence of pH on the adsorption of PANI/TiO_2 for ARG was significant. The adsorption stability experiments showed that in situ regeneration of PANI/TiO_2 was successfully achieved with NaOH as stripping agent, and HCl as activator. Adsorption equilibrium of PANI/TiO_2 for ARG could be achieved within 5 min. The adsorption kinetics of PANI/TiO_2 for ARG was interpreted well by the pseudo-second-order model, indicating the multiple adsorption mechanism of the PANI/TiO_2 adsorbent with saturated sites. According to the Langmuir adsorption isotherm model, the adsorption process was a monolayer adsorption and the maximum adsorption capacity of ARG on PANI/TiO_2 was 454.55 mg g^{-1}. In spite of regeneration for 8 times, PANI/TiO_2 still possessed excellent adsorption capacity for both the pure ARG solution and the real ARG effluent. It is expected that PANI/TiO_2 composites would have promising prospects on anion dye removal in wastewater treatment. The adsorption mechanism of the PANI/TiO_2 adsorbent was closely related to the doping/dedoping behaviors of the PANI chain on the nitrogen atoms, and may have nothing to do with the

special surface area. The adsorption of ARG on the composite can be considered as the substitution reaction of the counter ions on the protonated N atoms.

Acknowledgements

The authors gratefully acknowledge the financial supports from the National Natural Science Foundation of China (Grant No.21307098) and the Fundamental Research Funds for the Central Universities of China.

References

1 S.X. Xiong, S.L. Phua, B.S. Dunn, J. Ma, X.H. Lu, *Chem. Mater.*, 2010, **22**, 255-260.

2 J.J. Li, Q. Zhang, J.T. Feng, W. Yan, *Chem. Eng. J.*, 2013, **225**, 766-775.

3 L.B. Roberson, M.A. Poggi, J. Kowalik,, G.P. Smestad, L.A. Bottomley, L.M. Tolbert, *Coordin. Chem. Rev.*, 2004, **248**, 1491-1499.

4 G.F. Cai, J.P. Tu, D. Zhou, J.H. Zhang, Q.Q. Xiong, X.Y. Zhao, X.L. Wang, C.D. Gu, *J. Phys. Chem. C*, 2013, **117**, 15967-15975.

5 J.J. Li, J.T. Feng, W. Yan, *Appl. Surf. Sci.*, 2013, **279**, 400-408.

6 D. Mahanta, U. Manna, G. Madras, S. Patil. *Appl. Mat.interfaces*, 2011, **3**, 84-92.

7 W.D. Zhou, Y.C. Yu, H. Chen, F.J. DiSalvo, Héctor D. Abruña, *J. Am. Chem. Soc.*, 2013, **135**, 16736-16743.

8 A.L. Wang, H. Xu, J.X. Feng, L.X. Ding, Y.X. Tong, G.R. Li, *J. Am. Chem. Soc.*, 2013, **135**, 10703-10709.

9 S.G. Pawar, S.L. Patil, M.A. Chouugule, S.N. Achary, V.B. Patil, *Int. J. Polym. Mater.*, 2011, **60**, 244-254.

10 S. Sarmah, A. Kumar, *Indian J. Phys.*, 2011, 85,713-726.

11 P.P. Mahulikar, R.S. Jadhav, D.G. Hundiwale, *Iran. Polym. J.*, 2011, **20**, 367-376.

12 L.L. Xi, Z.Y. Zhu, F.L. Wang, *J. Electrochem. Soc.*, 2013, 160, 327-334.

13 Y. Zhu, J.M. Li, H.Y. He, M.X. Wan, L. Jiang, *Macromol. Rapid Commun.*, 2007, **28**, 2230-2236.

14 R. Ahmad, R. Kumar. *J. Chem. Eng. Data.*, 2010, 55, 3489-3493.

15 M. Ayad, S. Zaghlol. *Chem. Eng. J.*, 2012, 204-206, 79-86.

16 X.L. Tan, M. Fang, J.X. Li, Y. Lu, X.K. Wang, *J. Hazard.Mater.*, 2009, **168**, 458-465.

17 C.Q. Liu, L. Fu , James Economy, *J. Mater. Chem.*, 2004, **14**, 1187-1189.

18 N. Negishi, K. Takeuchi, T. Ibusuki, *J. Mat. Sci.*, 1998, **33**, 5789-5794.

19 G.H. Tian, H.G. Fu, L.Q. Jing, B.F. Xin, K. Pan, *J. Phys. Chem. C*, 2008, **112**, 3083-3089.

20 C. Perez Leon, L. Kador, B. Peng, M. Thelakkat, *J. Phys. Chem. B*, 2006, **110**, 8723-8730.

21 A. Zaban, S. Ferrere, B.A. Gregg, *J. Phys. Chem. B*, 1998, 102, 452-460.

22 I. Jang, K. Song, J.H. Park, S.G. Oh, Bull. *Korean Chem. Soc.*, 2013, 34, 2883-2888.

23 K. Bourikas, M. Stylidi, D.I. Kondarides, X.E. Verykios, Langmuir, 2005, 21, 9222-9230.

24 R. Giovannetti, M. Zannotti, L. Alibabaei, S. Ferraro, Int. J. Photoenergy, 2014, 2014, 1-9.

25 F. Zhang, F. Shi, W. Ma, F. Gao, Y. Jiao, H. Li, J.C. Wang, X.Y. Shan, X.H. Lu, S. Meng, *J. Phys. Chem. C*, 2013, **117**, 14659-14666.

26 P. Srivastava, S. Goyal, R. Tayade, *Can. J. Chem. Eng.*, 2014, **92**, 41-51.

27 M. Janus, J. Choina, A.W. Morawski, *J. Hazard. Mater.*, 2009, **166**, 1-5.

28 M. Janus, E. Kusiak, J. Choina, J. Ziebro, A.W. Morawski, Desalination, 2009, **249**, 359-363.

29 S. Asuha, X.G. Zhou, S. Zhao, *J. Hazard. Mater.*, 2010, **181**, 204-210.

30 T. Ishihara, Y. Misumi, H. Matsumoto, *Micropor. Mesopor. Mater.*, 2009, **122**, 87-92.

31 X.Y. Li, D.S. Wang, G.X. Cheng, Q.Z. Luo, J. An, Y.H. Wang, *Appl. Catal. B*, 2008, **81**, 267-273.

32 C.L. Aitken, W.J. Koros, D.R. Paul, *Macromolecules*, 1992, **25**, 3424-3434.

33 D. P. Wang, H.C. Zeng, *J. Phys. Chem. C*, 2009, **113**, 8097-8106.

34 J. Gong, Y.H. Li, Z.S. Hu, Z.Z. Zhou, and Y.L. Deng, *J. Phys. Chem. C*, 2010, **114**, 9970-9974.

35 M.R. Nabid, M. Golbabaee, A. Bayandori Moghaddam, R. Dinarvand, R. Sedghi, *Int. J. Electrochem. Sci.*, 2008, 3, 1117-1126.

36 S.H. Jang, M.G. Han, S.S. Im. *Synthetic Metals.*, 2000, 110, 17-23.

37 E.M. Geni ès, A. Boyle, M. Lapkowski, C. Tsintavis, *Synthetic Metals.*, 1990, 36, 139-182.

38 D.P. Wang, H.C. Zeng, *Chem. Mater.*, 2009, 21, 4811-4823.

39 J. Li, L.H. Zhu, Y.H. Wu, Y. Harima, A.Q. Zhang, H.Q. Tang, *Polymer.*, 2006, 47, 7361.

40 F. Deng, L.J. Min, X.B. Luo, S.L. Wu, S.L. Luo, Nanoscale, 2013, 5, 8703-8710.

41 G. Sonmez, H.B. Sonmez, C.K.F. Shen, F. Wudl, *Adv. Mater.*, 2004, 16, 1905-1908.

42 Y. Cheng, L. An, F. Gao, G.H. Wang, X.M. Li, X.Y. Chen, *Res. Chem. Intermed.*, 2013, 39, 3969-3979.

43 H.S. Xia, Q. Wang, *Chem. Mater.*, 2002, 14 , 2158-2165.

44 H.Z. Yu, M.G. Chen, H. Huang, Journal of South China University of Technology (Natural Science Edition), 2003, 31, 21-24.(in Chinese)

45 L. Ma, L.J. Feng, M.Y. Gan, X.S. Du, Chinese Journal of Applied Chemistry. 2008, 25, 142-146.

46 K.A.D. Guzman, M.P. Finnegan, J.F. Banfield, *Environ. Sci. Technol.*, 2006, 40, 7688-7693.

47 J. Wang, B.L. Deng, H. Chen, X.R. Wang, J.Z. Zheng, *Environ. Sci. Technol.*, 2009, 43, 5223-5228.

48 G.Z. Kyzas, J. Fu, K.A. Matis, *Materials*, 2013, 6, 5131-5158.

49 X. Zhang, R.B. Bai, *J. Mater. Chem.*, 2002, 12, 2733-2739.

50 Y.S. Ho, G. Mackay, *Process Biochem.*, 1999, 34, 451-465.

51 P. Xiong, L.J. Wang, X.Q. Sun, B.H. Xu, X. Wang, *Ind. Eng. Chem. Res.*, 2013, 52, 10105-10113.

52 Y.A. Zheng, Y. Liu, A.Q. Wang, *Ind. Eng. Chem. Res.*, 2012, 51, 10079-10087.

53 S.K. Li, X.F. Lu, Y.P. Xue, J.Y. Lei, T. Zheng, C. Wang, *PLos One.*, 2012, 7, 1-7.

54 L. Khezami, R. Capart, *J. Hazard. Mater. B*, 2005, 123, 223-231.

55 L. Bulgariu, D. Bulgariu, *J. Bioproces Biotechniq.*, 2014, 4, 2-8.

56 V. Gomez, M.S. Larrechi, M.P. Callao, *Chemosphere.*, 2007, 69, 1151-1158.

57 R.C. Wu, J.H. Qu, H. He, Y.B. Yu, *Appl. Catal. B: Environ.*, 2004, 48, 49-56.

58 D.S. Tong, C.H. Zhou, Y. Lan, H.Y. Yu, G.F. Zhang, W.H. Yu, *Appl. Clay Sci.*, 2010, 50, 427-431.

59 S. Tunali, A.S. Ozcan, A. Ozcan, *Hazard. Mater.*, 2006, 135, 141-148.

60 D. Mahanta, G. Madras, S. Radhakrishnan, and S. Patil, *J. Phys. Chem. B*, 2008, 112, 10153.

61 R. Ahmad and R. Kumar, *J. Chem. Eng. Data*, 2010, 55, 3489-3493.

62 J.A. Dean, Analytical chemistry handbook, McGRAW-HILL 1995

63 G.M. Nascimento, P.Y.G. Kobata, and M.L.A, Temperini, *J. Phys. Chem. B*., 2008, 112, 11551-11557.

64 M.Q. Sun, G.C. Wang, X.W. Li, Q.L. Cheng, and C.Z. Li, *J. Ind. Eng. Chem.*, 2012, 51, 3981-3987.

65 C'.M. Gordana, *Synth. Met.*, 2013, 177, 1-47.

66 C. Menardo, M. Nechtschein, A. Rousseau, J.P. Travers, *Synth. Met.*, 1988, 25, 311-322.

67 S. Bhadra, D. Khastgir, N.K. Singha, J.H. Lee, Prog. Polym. Sci. 2009, 34, 783-810.